Biocompatible and Flexible Chitosan-Based Resistive Switching Memory with Magnesium Electrodes

*Niloufar Raeis Hosseini and Jang-Sik Lee**

A flexible and transparent resistive switching memory based on a natural organic polymer for future flexible electronics is reported. The device has a coplanar structure of Mg/Ag-doped chitosan/Mg on plastic substrate, which shows promising nonvolatile memory characteristics for flexible memory applications. It can be easily fabricated using solution processes on flexible substrates at room temperature and indicates reliable memory operations. The elucidated origin of the bipolar resistive switching behavior is attributed to trap-related space-charge-limited conduction in high resistance state and filamentary conduction in low resistance state. The fabricated devices exhibit memory characteristics such as low power operation and long data retention. The proposed biocompatible memory device with transient electrodes is based on naturally abundant materials and is a promising candidate for low-cost memory applications. Devices with natural substrates such as chitosan and rice paper are also fabricated for fully biodegradable resistive switching memory. This work provides an important step toward developing a flexible resistive switching memory with natural polymer films for application in flexible and biodegradable nanoelectronic devices.

1. Introduction

Development of flexible electronics with electrical characteristics similar to those of rigid semiconductor devices would enable many novel uses involving wearable systems, e-papers, smart gloves, biointegrated medical devices, and electronic cameras on flexible substrates.[1–4] Electronic devices with organic/hybrid circuits on plastic substrates and mechanical flexibility also have obvious possible applications in the next generation of nanoelectronics.[5] Highly flexible circuit components have been established;[6] the ultimate goal is to fabricate rollable/bendable devices with high flexibility and stability of electrical properties.[2,7–9]

One of the important examples of a flexible circuit component is nonvolatile memory, which is an essential part in mobile electronics.[7,10,11] Achieving flexible nonvolatile memory is a major objective in the development of flexible electronics. Recently, nanoelectronic flexible resistive memories with stretchability,[12] bendability, and twistability[13] have been investigated.[14–19] Flexible resistive switching devices also have potential applications in implantable electronics.[16] Numerous researchers have presented memory technologies based on organics[20–22] and hybrid nanocomposites[23,24] for use in redox-based resistive switching memory (ReRAM) components.

Researchers are motivated to utilize organic molecules due to their alternative potential applications and compatibility with different plastic substrates.[25] Moreover, fabrication of organic-based ReRAMs is desirable in nonvolatile memory technology due to their flexibility[19,26,27] and transparency.[26,28] Organic polymers have also been used in resistive switching memory elements.[29–31] Furthermore, biopolymers are being considered for use in ReRAM due to their biocompatibility, disposability, low cost, and flexibility.[32–35]

The present research was conducted to extend previous achievements that used bioinspired materials in ReRAM devices.[36–39] Our previous work has examined the use of an abundant biomaterial, chitosan, in resistive switching memory applications.[40] Solid polymer electrolytes (SPEs) are suitable materials in thin film preparation due to their high flexibility and excellent processability.[31] SPEs have been developed because of their simple structure and facile operation in electrochemical switching memories.[31] Ag-doped chitosan has been suggested as a bioinspired SPE because of its ionic conductivity and biocompatibility.[40] Chitosan is a natural cationic polymer which is derived from chitin (Figure S1, Supporting Information).[41] Chitosan is nontoxic and biodegradable polysaccharide with different applications;[42] it has been introduced to fabricate a bioprotonic field-effect transistor.[43] In addition, chitosan was applied in indium-zinc-oxide (IZO)-based transistors to imitate synaptic plasticity.[44] Chitosan-based thin film is homogeneous with low electrical conductivity and high mechanical strength.[45] The ionic conductivity of chitosan can be increased by adding salts and plasticizers.[46]

In our system, $AgNO_3$ was selected as the additive salt; NH_2 groups in the chitosan react with metal ions because the N atoms have free electron doublets.[47] Chitosan-based thin film has the additional advantages of being transparent and uniform; these traits are important when fabricating a transparent flexible memory device. Building on previous studies, we propose a solution-based biological natural material as the SPE of a nonvolatile organic memory device. We also present use of Mg

---

N. Raeis Hosseini, Prof. J.-S. Lee
Department of Materials Science and Engineering
Pohang University of Science and Technology
(POSTECH)
Pohang 790-784, South Korea
E-mail: jangsik@postech.ac.kr

DOI: 10.1002/adfm.201502592

as a biocompatible and transient electrode for nonvolatile resistive switching memory devices. Mg was selected as a candidate ReRAM electrode in bio SPE-based devices because of its availability and recyclability as well as good electrical conductivity.[48]

As a basic requirement, long-lasting physical stability of nanoelectronic memory devices is a significant characteristic for real application. However, wearable and implantable devices need to work in a scheduled time with their predefined function and then to be decomposed in the environment or to be absorbed to body skin.[49] To fabricate electronic devices with transient properties, several parameters were taken into account. First, among different electrode materials we selected Mg due to its biodegradability and electrical conductivity. Furthermore, the material selection was accomplished by considering the degradability of chitosan and Mg as transient switching material and electrode, respectively. The transient behaviors are essential in medical diagnostic applications and healing devices which needs to get absorbed to body to reduce consecutive surgeries.[50] In addition, recyclable and decomposable devices are beneficial to reduce the costs and health risks by semiconductor residues.[49] The biodegradable and transient ReRAMs using natural materials have potential application in medicine for implantable devices and green/eco-friendly consumer electronics.[50]

We suggest a flexible transient ReRAM device utilizing a biopolymer with compatibility on a variety of substrates like polyethylene terephthalate (PET), chitosan, and rice paper. The major advantage of chitosan compared to other organics is that chitosan is a biodegradable and edible natural material which can also be applied to heal wounds due to its compatibility on human skin. In our cost-effective system, we also reduced the electrode deposition steps using coplanar structure to decrease the device fabrication process cost with minimizing the quantity of required materials. We represent a flexible biodegradable ReRAM device that has chitosan as the resistive switching layer and Mg as the electrode. We also introduce an inexpensive and vacuum-free solution process to fabricate a transparent flexible memory device that can be utilized in emerging electronic devices.

2. Results and Discussion

The memory effect of the Ag-doped chitosan-based resistive switching device was studied by using devices fabricated onto indium-tin oxide (ITO)-coated PET flexible substrates. An Ag-doped chitosan solution was applied to the substrate by spin coating, and then fabrication was completed by thermal evaporation of Mg electrodes on the dried SPE thin film through shadow masks. A Mg/Ag-doped chitosan layer/Mg structure was used to demonstrate the memory device with a coplanar capacitor structure (**Figure 1**a,b). The fabricated devices were flexible and transparent (Figure 1b).

Electrical characterizations of the chitosan-based ReRAM were performed at room temperature; the measured current–voltage relationship (*I*–*V*) presents typical resistive switching behavior (**Figure 2**a). To measure the *I*–*V* responses of the Mg/Ag-doped chitosan/Mg device, the voltage was controlled by one of the Mg electrodes under dc sweeping voltage applied as 0 V → 2 V → 0 V → −3 V → 0 V, while the other Mg electrode was grounded. During the first voltage sweep (upon applying the positive bias) from zero to set voltage ($V_{set} \approx 1.5$ V), the resistance state was changed from its pristine state to a conductive ON state. A compliance current of 5×10^{-4} A was used to prevent device breakdown. Subsequently applying a voltage of opposite polarity changed the resistance state back to the insulative OFF state (Figure 2a). A subsequent ON state was reproduced by applying positive voltage to reach the SET process. A data retention test was performed to appraise the stability of the memory device with a reading bias of 0.14 V under ambient condition. An acceptably high ON/OFF ratio ($>10^2$) was achieved in the chitosan-based ReRAM device, and no discernible degradation in the current of low resistance state (LRS) and high resistance state (HRS) was observed over 10^4 s; this stability indicates that the device provides nonvolatile memory property (Figure 2b). The reliability of resistive switching in the chitosan-based devices was confirmed by its endurance property with repeated cyclic tests. There is no noticeable degradation in endurance property for over 60 dc cycles (Figure 2c); this result implies the robustness of the memory performance. We determined the cumulative distribution of set and reset voltages. The average required voltages to accomplish set and reset operations were found to be around 1.63 V and −0.82 V, respectively (Figure 2d).

In mechanical flexibility tests with 5 mm radius of curvature for 1000 cycles at readout voltage of 0.14 V both ON and OFF currents remained stable (**Figure 3**a). We also examined the *I*–*V* characteristics of Mg/Ag-doped chitosan/Mg under tensile (Figure 3b)

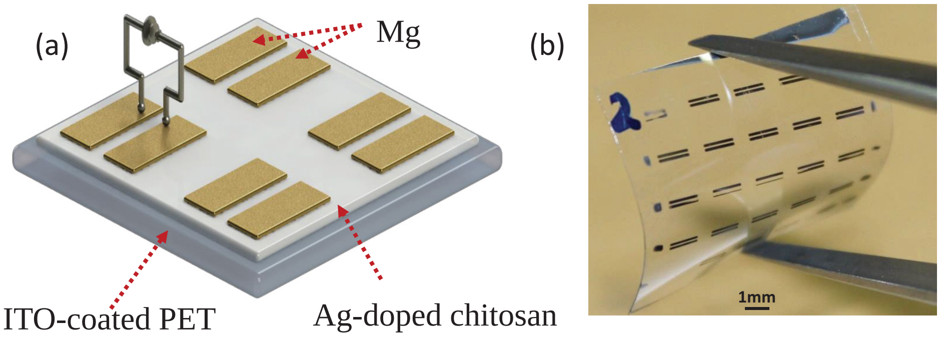

Figure 1. a) Schematic illustration of Mg/Ag-doped chitosan/Mg device structures and b) photograph of the flexible and biocompatible memory devices.

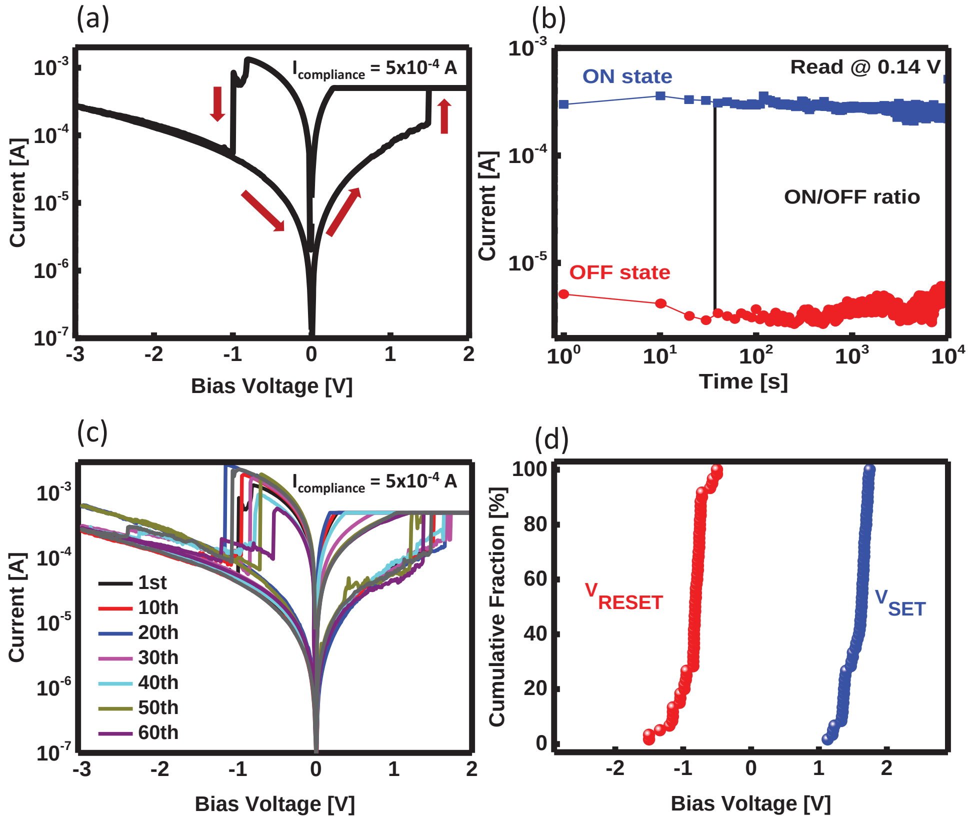

Figure 2. a) *I*–*V* characteristics of the Mg/Ag-doped chitosan/Mg resistive switching memory device. Current compliance of 5×10^{-4} A was applied to prevent permanent breakdown. b) Data retention characteristics of LRS and HRS states under continuous readout voltage at room temperature. c) Switching endurance of the chitosan-based memory device measured up to 60 cycles. d) Cycle-to-cycle statistical cumulative distribution of the SET and RESET voltages.

and compressive stresses (Figure 3c) by bending the devices with 5 mm radius of curvature. These results reveal that the flexible memory devices exhibit reliable nonvolatile memory properties with definite memory behaviors including retention, endurance, ON/OFF current ratio, and good uniformity for memory operation. To confirm the transparency of our device, UV–vis transmittance spectra were recorded for an Ag-doped chitosan thin film on the plastic substrate. The transmittance was about 86% at a wavelength of 450 nm (Figure S2, Supporting Information).

The resistive switching mechanism transition from a trap-induced space-charge-limited conduction (SCLC) mechanism to a conductive filament creation and destruction is specified by various characteristics in a semilogarithmic *I*–*V* curve (**Figure** 4a). To elucidate the conduction mechanism in the switching layer of the Mg/Ag-decorated chitosan/Mg memory device, double logarithmic plots of the *I*–*V* curves for the positive and negative voltage sweep regions were obtained (Figure 4b,c). The fitting result of LRS and HRS currents implies that in the HRS region the current conduction in the SPE layer is SCLC, but in the LRS region the carrier transport is dominated by ohmic conduction and current conduction is of a filamentary type (Figure 4b,c). We believe that the SCLC mechanism occurs due to traps generated by dopants/trap sites in the Ag-doped chitosan thin film. In the 0 V → 2 V regime, the *I*–*V* curves showed two distinct sections; the curve was linear at lower voltage regime (blue line), and then almost quadratic (red line) until set voltage was reached. At low voltage the electric field across the device is not sufficient, so the number of injected charge carriers is less than the number of thermally generated free charge carriers;[37,51] therefore the *I*–*V* characteristics obeyed Ohm's law ($I \propto V$) (Figure 4b). At higher voltage the trap centers become occupied by abundant charge carriers due to increased voltage.[52–55] Accordingly, the conduction mechanism of the HRS shows IV^2 dependency (square-law dependency on voltage), which is consistent with SCLC. SCLC nature is governed by traps and the ratio of free carriers to trapped ones.[52–55] When voltage was swept from +2 V → 0 V, the *I*–*V* characteristics were linear (slope of ≈ 0.95, brown line), which suggests that the conduction involves filamentary path. When the bias was negative, the logarithmic *I*–*V* curve in LRS was similar to the +2 V → 0 V bias; during the voltage sweep from −3 V → 0 V, the transition between SCLC-controlled conduction and ohmic conduction occurred (Figure 4c). To compare the performance of the Mg electrode with other electrode materials, we fabricated flexible ReRAM devices with coplanar Al and Ag electrodes. Current–voltage responses of the Mg/Ag-doped chitosan/Mg device are comparable with other electrode materials like Al and Ag (Figure S3, Supporting Information).

To evaluate the transient behavior of Mg electrodes, we dropped deionized (DI) water on the fabricated device and observed the time-dependent dissolution of transient electrodes at room temperature (**Figure** 5a–d). After dropping water on the

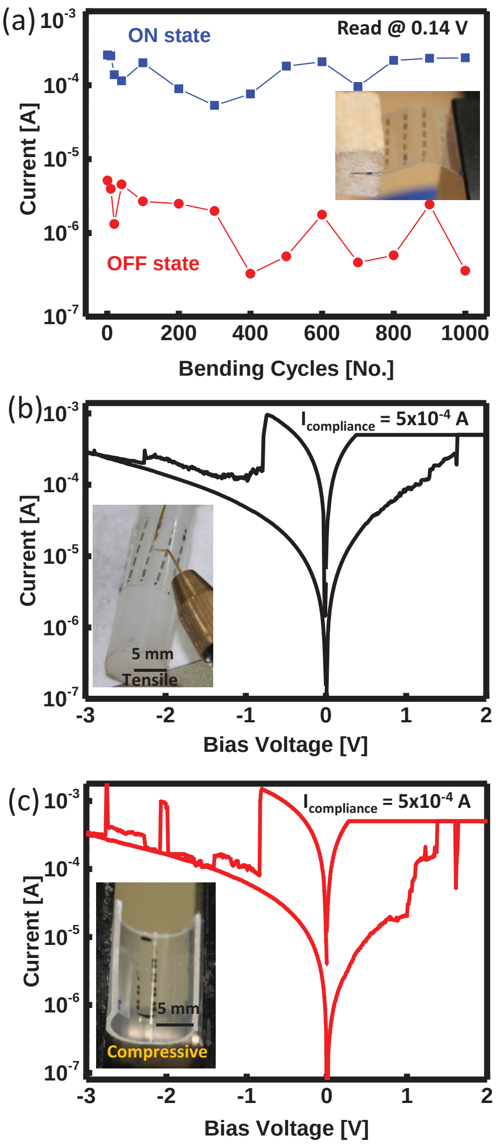

Figure 3. a) Mechanical bending stability of chitosan-based flexible resistive switching memory devices. The current levels of ON and OFF states were measured after repetitive bending cycles. The devices were bent with a radius of curvature of 5 mm; inset: curved devices attached to bending test facility. *I–V* characteristics of Mg/Ag-doped chitosan/Mg under b) tensile and c) compressive bending with a radius of curvature of 5 mm; inset: photograph of the bent device used for measurement.

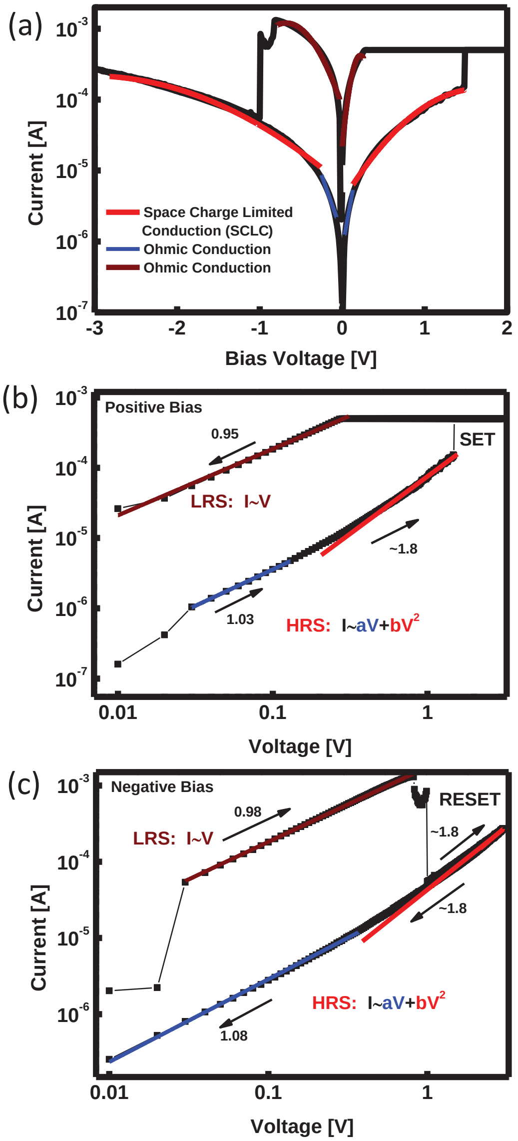

Figure 4. Experimental and fitted *I–V* curves of the Mg/Ag-doped chitosan/Mg resistive switching memory device: a) Semilogarithmic *I–V* curve with fitted models; double-logarithmic plot with the space-charge-limited model in b) positive and c) negative sweep. The values of slopes are listed in the plots.

electrodes, Mg started reacting with water and got consumed by hydrolysis. It has been observed that Mg is totally dissolved in water after 1.5 h. It is possible to prevent the decomposition of Mg electrodes by passivation of the devices using atomic-layer deposited (ALD) Al_2O_3 thin films. Upon dropping water on the Mg electrodes, decomposition is done easily as already observed in Figure 5, while the coated devices show almost no change in Mg electrodes (Figure S4, Supporting Information). Simple passivation using a thin oxide layer prevents the decomposition and can be used to fabricate devices for extended use.

To fabricate fully biocompatible and biodegradable memory devices, the key challenge is the utilization of biodegradable substrates. We demonstrated the possibility of fabricating memory devices on biodegradable substrates: rice paper and chitosan. Rice paper is food which can be utilized as a substrate as well for edible and decomposable electronic devices.[49] We deposited the memory device components on rice paper (Figure S5, Supporting Information). Each component dissolves well under water drop. We also fabricated completely decomposable devices, where chitosan thick layers served as the substrate while Mg was used as the electrode. Chitosan is utilized as the substrate for green electronic devices. As can be seen in **Figure 6**, the deposition of Mg on a chitosan substrate was successfully done by evaporation. The collected images during dissolution of chitosan substrates and Mg electrodes after dropping DI water showed gradual vanishing of the electrodes and substrates

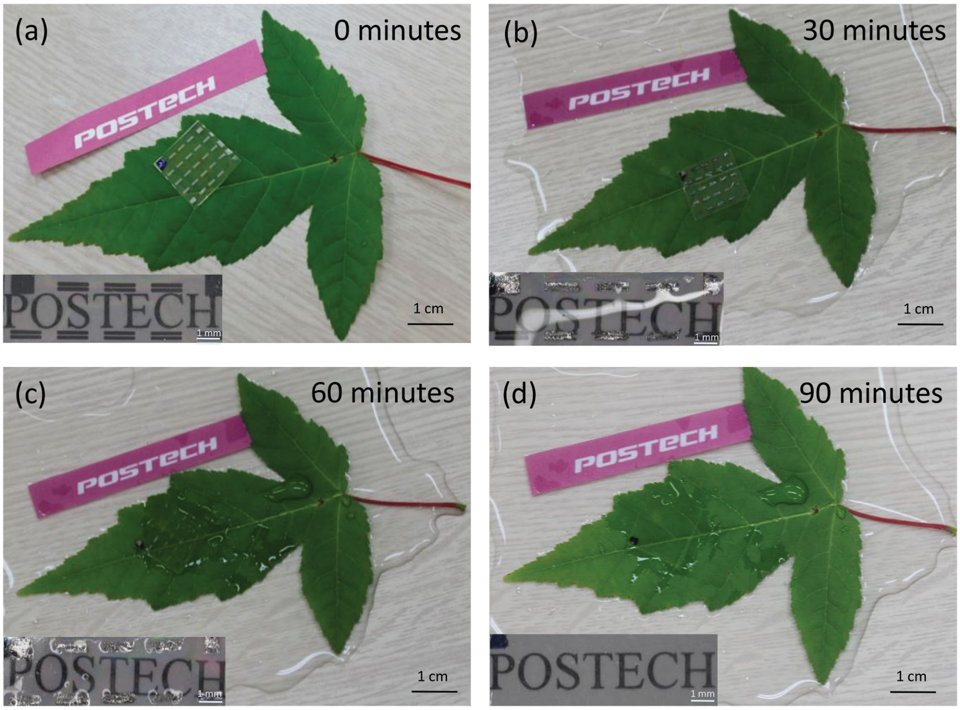

Figure 5. Evolution of Mg electrodes with water at room temperature using fabricated memory of Mg/Ag-doped chitosan/Mg on the plastic substrate according to the elapsed time. a) Before dropping water, b) 30 min, c) 60 min, and d) 90 min after dropping DI water on the devices; inset: magnified optical images of the reaction of Mg electrodes with water.

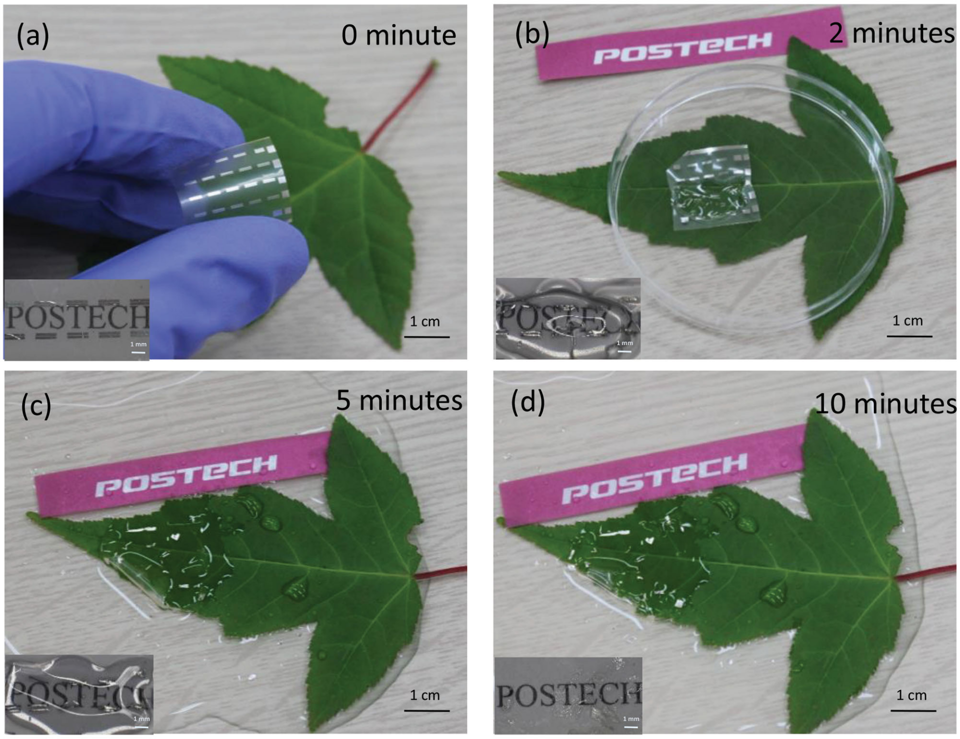

Figure 6. Biodegradable and decomposable devices made of chitosan as the substrate with coplanar Mg electrodes. a) Fabricated transparent and flexible devices. Decomposition of devices after dropping water in b) 2 min, c) 5 min, and d) 10 min; inset: magnified optical images of the gradual decomposition of chitosan-based devices.

until total decomposition. Mg electrodes reacted with water and decomposed. In addition, chitosan absorbed water and was deformed until the devices were finally vanished (Figure 6a–d). We compared this work with previous biocompatible material-based ReRAM devices (Table S1, Supporting information).

3. Conclusion

We investigated biocompatible and flexible resistive switching memory devices based on chitosan as the natural SPE layer on the transparent and bendable substrate. We demonstrated the resistive switching characteristics of ReRAM with bipolar switching properties for nonvolatile flexible memory applications. The device was fabricated by solution processes using chitosan biopolymers dissolved in dilute acetic acid. The device can be switched with a reasonable ON/OFF current ratio ($>10^2$) and low operation voltages with good mechanical reliability. In addition, the transparent and flexible chitosan-based ReRAM with Mg electrodes shows good retention capability ($\approx 10^4$ s). Based on the obtained results, the fabricated chitosan-based organic memory with Mg electrodes is highly promising for use in flexible, low cost, low power, and biodegradable memory applications. It also has a good potential to be used in inexpensive and environmentally benign flexible memory devices. The switching behavior is attributed to trap controlled SCLC and metallic filament formation in HRS and LRS, respectively. Consequently, our device represents reproducible resistive switching behavior under applied electrical biases with eco-friendly and biocompatible properties.

4. Experimental Section

Materials and Device Fabrication: The ReRAM devices with a coplanar structure of Mg/SPE/Mg were fabricated on ITO-coated PET flexible substrates. The PET substrates were ultrasonically cleaned using acetone, 2-propanol, and distilled water for 15 min, and then dried using N_2 gas. A crab shell-based chitosan with a medium molecular weight (deacetylation degree 75%–85%, Sigma-Aldrich) was dissolved (1% w/v) in 1% acetic acid solution in distilled water, and mixed overnight under ambient temperature and constant stirring at 120rpm. The solution was filtered through 0.4 µm PVDF syringe filters. $AgNO_3$ powder (99.9999%, Sigma-Aldrich) was mixed with the chitosan solution at 1 wt%; then the resulting solution filtered through a 0.2 µm PVDF filter. The obtained solution was spin coated on the transparent and flexible substrate at 500 rpm for 5 s and 1200 rpm for 25 s. The Ag-doped chitosan film was dried at ambient temperature overnight, then Mg electrodes were patterned using thermal evaporation to make a coplanar ReRAM device with a 23 µm gap between the electrodes. The coplanar ReRAM devices with Ag and Al electrodes were fabricated with the same way as those for Mg/SPE/Mg devices using thermal evaporation. For the device passivation Al_2O_3 thin film was deposited by ALD at 140 °C using trimethylaluminium and O_2 plasma. The disposable devices with rice paper substrate were fabricated by drop-casting of Ag-doped chitosan on the rice paper following the deposition of Mg electrodes by evaporation. The decomposable device using chitosan as the substrate was prepared by filtering the chitosan-acetate 1 wt% solution through 0.2 µm PVDF filters and casting it on a petri dish. After debubbling the casting solution for 1 h under vacuum condition in a vacuumed desiccator at room temperature, it was maintained in a vacuum oven at 50 °C for 8 h to become a robust membrane. The device fabrication was accomplished by thermal evaporation of Mg electrodes using coplanar shadow mask.

Characterization: A Cary 100 UV–vis spectrophotometer (Agilent Technologies, CA, USA) equipped with transmittance accessory was used to record the optical spectrum of the samples over the wavelength range of 200–800 nm. The transmittance spectra were collected from Ag-doped chitosan thin films on the plastic substrate. Electrical characteristics of the fabricated devices were analyzed at atmospheric pressure under ambient temperature using a semiconductor parameter analyzer (Keithley 4200SCS, USA) for applying voltage and measuring current. In a typical test configuration, the sample was placed in a probe station, and bias voltages were applied to one of the Mg electrodes while the other electrode was grounded.

Supporting Information

Supporting Information is available from the Wiley Online Library or from the author.

Acknowledgements

This work was supported by the Future Semiconductor Device Technology Development Program (10045226) funded by the Ministry of Trade, Industry and Energy (MOTIE), and the Korea Semiconductor Research Consortium (KSRC); by the National Research Foundation (NRF) grant funded by the Korea government (MEST) (2010-0015014). In addition, this work was partially supported by the Brain Korea 21 PLUS project (Center for Creative Industrial Materials).

Received: June 24, 2015

---

[1] R. H. Reuss, B. R. Chalamala, A. Moussessian, M. G. Kane, A. Kumar, D. C. Zhang, J. Rogers, M. Hatalis, D. Temple, G. Moddel, *Proc. IEEE* **2005**, *93*, 1239.
[2] M. Kaltenbrunner, T. Sekitani, J. Reeder, T. Yokota, K. Kuribara, T. Tokuhara, M. Drack, R. Schwodiauer, I. Graz, S. Bauer-Gogonea, S. Bauer, T. Someya, *Nature* **2013**, *499*, 458.
[3] C. Zysset, N. Munzenrieder, L. Petti, L. Buthe, G. A. Salvatore, G. Troster, *IEEE Electron Device Lett.* **2013**, *34*, 1394.
[4] U. Zschieschang, T. Yamamoto, K. Takimiya, H. Kuwabara, M. Ikeda, T. Sekitani, T. Someya, H. Klauk, *Adv. Mater.* **2011**, *23*, 654.
[5] G. Yang, Y. Jung, C. V. Cuervo, F. Ren, S. J. Pearton, J. Kim, *Opt. Express* **2014**, *22*, A812.
[6] H. Kang, S. Jung, S. Jeong, G. Kim, K. Lee, *Nat. Commun.* **2015**, *6*, 6503.
[7] T. Sekitani, T. Yokota, U. Zschieschang, H. Klauk, S. Bauer, K. Takeuchi, M. Takamiya, T. Sakurai, T. Someya, *Science* **2009**, *326*, 1516.
[8] R.-H. Kim, D.-H. Kim, J. Xiao, B. H. Kim, S.-I. Park, B. Panilaitis, R. Ghaffari, J. Yao, M. Li, Z. Liu, *Nat. Mater.* **2010**, *9*, 929.
[9] T. Sekitani, U. Zschieschang, H. Klauk, T. Someya, *Nat. Mater.* **2010**, *9*, 1015.
[10] H. C. Chang, C. L. Liu, W. C. Chen, *Adv. Funct. Mater.* **2013**, *23*, 4960.
[11] S. T. Han, Y. Zhou, Z. X. Xu, L. B. Huang, X. B. Yang, V. Roy, *Adv. Mater.* **2012**, *24*, 3556.
[12] D.-H. Kim, J.-H. Ahn, W. M. Choi, H.-S. Kim, T.-H. Kim, J. Song, Y. Y. Huang, Z. Liu, C. Lu, J. A. Rogers, *Science* **2008**, *320*, 507.
[13] Y. Ji, D. F. Zeigler, D. S. Lee, H. Choi, A. K. Y. Jen, H. C. Ko, T.-W. Kim, *Nat. Commun.* **2013**, *4*, 2707.

[14] D. I. Son, T. W. Kim, J. H. Shim, J. H. Jung, D. U. Lee, J. M. Lee, W. I. Park, W. K. Choi, *Nano Lett.* **2010**, *10*, 2441.
[15] D. I. Son, J. H. Shim, D. H. Park, J. H. Jung, J. M. Lee, W. I. Park, T. W. Kim, W. K. Choi, *Nanotechnology* **2011**, *22*, 295203.
[16] H. Y. Jeong, J. Y. Kim, J. W. Kim, J. O. Hwang, J.-E. Kim, J. Y. Lee, T. H. Yoon, B. J. Cho, S. O. Kim, R. S. Ruoff, *Nano Lett.* **2010**, *10*, 4381.
[17] J. Liu, Z. Yin, X. Cao, F. Zhao, L. Wang, W. Huang, H. Zhang, *Adv. Mater.* **2013**, *25*, 233.
[18] J. Yun, K. Cho, B. Park, B. H. Park, S. Kim, *J. Mater. Chem.* **2009**, *19*, 2082.
[19] Y. Ji, B. Cho, S. Song, T. W. Kim, M. Choe, Y. H. Kahng, T. Lee, *Adv. Mater.* **2010**, *22*, 3071.
[20] B. Cho, J. M. Yun, S. Song, Y. Ji, D. Y. Kim, T. Lee, *Adv. Funct. Mater.* **2011**, *21*, 3976.
[21] C. Kügeler, M. Meier, R. Rosezin, S. Gilles, R. Waser, *Solid-State Electron.* **2009**, *53*, 1287.
[22] I. Valov, R. Waser, *J. Phys. Chem. C* **2013**, *117*, 11878.
[23] S. H. Jo, K.-H. Kim, W. Lu, *Nano Lett.* **2008**, *9*, 496.
[24] T. W. Kim, Y. Yang, F. Li, W. L. Kwan, *NPG Asia Mater.* **2012**, *4*, e18.
[25] S. R. Forrest, *Nature* **2004**, *428*, 911.
[26] H.-D. Kim, M. J. Yun, J. H. Lee, K. H. Kim, T. G. Kim, *Sci. Rep.* **2014**, *4*, 4614.
[27] T. Lee, Y. Chen, *MRS Bull.* **2012**, *37*, 144.
[28] J. Yao, J. Lin, Y. Dai, G. Ruan, Z. Yan, L. Li, L. Zhong, D. Natelson, J. M. Tour, *Nat. Commun.* **2012**, *3*, 1101.
[29] W. P. Lin, S. J. Liu, T. Gong, Q. Zhao, W. Huang, *Adv. Mater.* **2014**, *26*, 570.
[30] S. Song, B. Cho, T. W. Kim, Y. Ji, M. Jo, G. Wang, M. Choe, Y. H. Kahng, H. Hwang, T. Lee, *Adv. Mater.* **2010**, *22*, 5048.
[31] S. Wu, T. Tsuruoka, K. Terabe, T. Hasegawa, J. P. Hill, K. Ariga, M. Aono, *Adv. Funct. Mater.* **2011**, *21*, 93.
[32] M. Irimia-Vladu, E. D. Głowacki, G. Voss, S. Bauer, N. S. Sariciftci, *Mater. Today* **2012**, *15*, 340.
[33] M. K. Hota, M. K. Bera, B. Kundu, S. C. Kundu, C. K. Maiti, *Adv. Funct. Mater.* **2012**, *22*, 4493.
[34] Y.-C. Hung, W.-T. Hsu, T.-Y. Lin, L. Fruk, *Appl. Phys. Lett.* **2011**, *99*, 253301.
[35] F. Meng, L. Jiang, K. Zheng, C. F. Goh, S. Lim, H. H. Hng, J. Ma, F. Boey, X. Chen, *Small* **2011**, *7*, 3016.
[36] N. Gogurla, S. P. Mondal, A. K. Sinha, A. K. Katiyar, W. Banerjee, S. C. Kundu, S. K. Ray, *Nanotechnology* **2013**, *24*, 345202.
[37] H. Wang, F. Meng, Y. Cai, L. Zheng, Y. Li, Y. Liu, Y. Jiang, X. Wang, X. Chen, *Adv. Mater.* **2013**, *25*, 5498.
[38] K. Nagashima, H. Koga, U. Celano, F. Zhuge, M. Kanai, S. Rahong, G. Meng, Y. He, J. De Boeck, M. Jurczak, W. Vandervorst, T. Kitaoka, M. Nogi, T. Yanagida, *Sci. Rep.* **2014**, *4*, 5532.
[39] Y.-C. Chen, H.-C. Yu, C.-Y. Huang, W.-L. Chung, S.-L. Wu, Y.-K. Su, *Sci. Rep.* **2015**, *5*, 10022.
[40] H. N. Raeis, J.-S. Lee, *ACS Nano* **2015**, *9*, 419.
[41] S. Boddohi, M. J. Kipper, *Adv. Mater.* **2010**, *22*, 2998.
[42] M. Yahya, A. Arof, *Eur. Polym. J.* **2003**, *39*, 897.
[43] C. Zhong, Y. Deng, A. F. Roudsari, A. Kapetanovic, M. Anantram, M. Rolandi, *Nat. Commun.* **2011**, *2*, 476.
[44] J. Zhou, Y. Liu, Y. Shi, Q. Wan, *IEEE Electron Device Lett.* **2014**, *35*, 280.
[45] A. S. A. Khiar, R. Puteh, A. K. Arof, *Phys. B: Condens. Matter* **2006**, *373*, 23.
[46] N. Morni, N. Mohamed, A. Arof, *Mater. Sci. Eng.: B* **1997**, *45*, 140.
[47] E. Guibal, *Sep. Purif. Technol.* **2004**, *38*, 43.
[48] B. Mordike, T. Ebert, *Mater. Sci. Eng.: A* **2001**, *302*, 37.
[49] S.-W. Hwang, H. Tao, D.-H. Kim, H. Cheng, J.-K. Song, E. Rill, M. A. Brenckle, B. Panilaitis, S. M. Won, Y.-S. Kim, *Science* **2012**, *337*, 1640.
[50] S. W. Hwang, J. K. Song, X. Huang, H. Cheng, S. K. Kang, B. H. Kim, J. H. Kim, S. Yu, Y. Huang, J. A. Rogers, *Adv. Mater.* **2014**, *26*, 3905.
[51] B. Zeng, D. Xu, M. Tang, Y. Xiao, Y. Zhou, R. Xiong, Z. Li, Y. Zhou, *J. Appl. Phys.* **2014**, *116*, 124514.
[52] S. Mondal, J.-L. Her, F.-H. Chen, S.-J. Shih, T.-M. Pan, *IEEE Electron Device Lett.* **2012**, *33*, 1069.
[53] P. Feng, C. Chao, Z.-S. Wang, Y.-C. Yang, Y. Jing, Z. Fei, *Prog. Nat. Sci.: Mater. Int.* **2010**, *20*, 1.
[54] D. Shang, Q. Wang, L. Chen, R. Dong, X. Li, W. Zhang, *Phys. Rev. B* **2006**, *73*, 245427.
[55] S. Chithiravel, K. Krishnamoorthy, S. Asha, *J. Mater. Chem. C* **2014**, *2*, 9882.